



Published in final edited form as:

Biomaterials. 2015 May ; 51: 51–57. doi:10.1016/j.biomaterials.2015.01.033.

Mussel adhesive protein provides cohesive matrix for collagen type-1 α

Nadine R. Martinez Rodriguez^a, Saurabh Das^b, Yair Kaufman^b, Wei Wei^c, Jacob N. Israelachvili^{b,c,1}, and J. Herbert Waite^{b,c,d,1}

^aDepartment of Molecular, Cell & Developmental Biology, University of California, Santa Barbara, California 93106, USA

^bDepartment of Chemical Engineering, University of California, Santa Barbara, California 93106, USA

^cMaterials Research Laboratory, University of California, Santa Barbara, California 93106, USA

^dDepartment of Chemistry and Biochemistry, University of California, Santa Barbara, California 93106, USA

Abstract

Understanding the interactions between collagen and adhesive mussel foot proteins (mfps) can lead to improved medical and dental adhesives, particularly for collagen-rich tissues. Here we investigated interactions between collagen type-1, the most abundant loadbearing animal protein, and mussel foot protein-3 (mfp-3) using a quartz crystal microbalance and surface forces apparatus (SFA). Both hydrophilic and hydrophobic variants of mfp-3 were exploited to probe the nature of the interaction between the protein and collagen. Our chief findings are: 1) mfp-3 is an effective chaperone for tropocollagen adsorption to TiO₂ and mica surfaces; 2) at pH 3, collagen addition between two mfp-3 films ($W_c = 5.4 \pm 0.2$ mJ/m²) increased their cohesion by nearly 35%; 3) oxidation of Dopa in mfp-3 by periodate did not abolish the adhesion between collagen and mfp-3 films, and 4) collagen bridging between both hydrophilic and hydrophobic mfp-3 variant films is equally robust, suggesting that hydrophobic interactions play a minor role. Extensive H-bonding, π -cation and electrostatic interactions are more plausible to explain the reversible bridging of mfp-3 films by collagen.

Keywords

mussel foot proteins; collagen type-1; mfp-3

© 2015 Published by Elsevier Ltd.

¹Corresponding authors: jacob@engineering.ucsb.edu, Phone: (805) 893-8407, Fax: (805) 893-7870. waite@lifesci.ucsb.edu, Phone: (805) 893-2817.

Publisher's Disclaimer: This is a PDF file of an unedited manuscript that has been accepted for publication. As a service to our customers we are providing this early version of the manuscript. The manuscript will undergo copyediting, typesetting, and review of the resulting proof before it is published in its final citable form. Please note that during the production process errors may be discovered which could affect the content, and all legal disclaimers that apply to the journal pertain.

Introduction

Collagen is the most abundant protein family in animals and is present to some extent in all tissues of the body ranging from about 6 mg/g wet weight in healthy liver to 300 mg/g in tendon [1, 2]. The collagen family is a diverse one with over 28 different known types all sharing the Gly-X-Y tripeptide repeat motif and left-handed triple helices, but differing in the number of aberrations from the Gly-X-Y repeat and by the presence and size of non-collagenous domains [3]. The functions of collagen are manifold but there is general agreement that collagen contributes critically to the load-bearing properties of most if not all tissues [4]. However strong they may be, collagen-rich tissues are prone to damage, and after injury, heal at best slowly in bone and tendon [5] or not at all as in dentin [6]. Given this, it is surprising that few studies have specifically targeted collagen *in situ* in injured tissues for repair [7, 8].

Mussel adhesive proteins (mfps) have an intriguing potential for repair of collagenous tissues in that, in the byssal attachment plaques, they mediate adhesion between the collagens of the thread on one side and a foreign surface on the other (Fig. 1a). Measuring the adhesion between collagens and mfps has not been done before and is challenging because collagen mediated adhesion between inert surfaces is weak [9] and because tethering chemistries often result in collagen denaturation. In the present study adhesion was inspired by the structure of the adhesive plaque, which is essentially an A-B-C joint in which A is collagen, B denotes the adhesive mfps and C is mica (Fig. 1). Because mfp-3 adhesion is adaptable to many surfaces [10], we hypothesized that the test specimen in a surface forces apparatus could be configured as a C-B-A-B-C joint (Fig. 1b) [11]. If the C-B interface remained the strongest interaction, then it should be possible, in principle, to independently assess the interaction between mfp-3 films mediated by collagen. Indeed, our studies at pH 3 have shown that addition of collagen type 1 α increased the cohesion between mfp-3 films. Adhesive molecules that can reconnect collagens in damaged tissues or attach collagens to biomineral or implant surfaces have a wide-ranging potential to benefit health care delivery in surgery, dentistry, and pharmaceutical products.

Results and Discussion

Collagen adsorption with and without mfp-3

We investigated the adhesive interactions between tropocollagen type-1 (COL1A1) and mfp-3 by three different techniques: (1) QCM-D to measure the co-adsorption of COL1A1 and mfp-3 to titania surfaces, (2) AFM to investigate the topography of COL1A1 to mfp-3 film on a mica surface, and (3) to measure the bridging interactions of collagen type-1 (COL1A1) between symmetric mfp-3 films using a surface forces apparatus (SFA). We used two different variants of mfp-3, mfp-3 fast (mfp-3f, hydrophilic) and mfp-3 slow (mfp-3s, hydrophobic), to test the effect of hydrophobicity on the interaction between the proteins and COL1A1. The fast (f) and slow (s) aspects of the acronym simply refer to the characteristic chromatographic elution times of the two variants during purification. Both mfp-3f and mfp-3s have low molecular weights (~5–7 kDa) and highly homologous sequences. However, mfp-3s has less than half the charge density of Mfp-3f making it significantly more hydrophobic than mfp-3f. Although both variants contain Dopa, all Tyr

residues are post-translationally modified in mfp-3f, whereas only 60% are modified in mfp-3s [12].

Sequential adsorption of Mfp-3 and COL1A1 to TiO₂ using QCM-D

Collagen type-1 is the major protein in human connective tissue including skin, tendon, ligament, bone, and tooth dentin. In the present study, pure rat-tail tropocollagen (COL1A1) was used because of its long uninterrupted triple helical domain (preCOL-D, in contrast, has six different domains, the largest one of which is triple helical). QCM-D was used to investigate the adsorption of COL1A1 to mfp-3 pre-adsorbed to a TiO₂ coated (top-layer) sensor surface (Fig. S1). QCM was also used to demonstrate the adsorption of *hydrated* COL1A1 to a TiO₂ surface assisted by mfp-3 (Fig. 3). A previous study [13] based on both Surface Plasmon Resonance (SPR) and QCM demonstrated hydration in mfp-1 adsorbed to quartz to be substantial ~95% and decrease upon cross-linking. For the purpose of this study we assumed protein hydration to remain unchanged. TiO₂ surfaces and not mica were used for the QCM-D adsorption experiments since TiO₂ coated crystal surfaces are commercially available and have been previously used for the study of mfp-3s adsorption experiments [14]. It has been also previously demonstrated that the interactions between mfp-3 and mica or TiO₂ are similar: both surfaces interact with mfp-3 through H-bonding at low pH and the crystal structure of the two surfaces at the water-surface interface has a geometry commensurate with bidentate H-bonding interactions [15].

Mfp-3 fast (hydrophilic) or slow (hydrophobic) was injected onto a TiO₂ surface in 0.1 M sodium acetate buffer, pH 3.0 and 0.25 M KNO₃. The acidic pH was used to prevent the aggregation of tropocollagen. The frequency change, F , is proportional to the mass of the adsorbed molecules and it is clear that mfp-3f and mfp-3s adsorbed ($m \sim 217$ and ~ 274 ng/cm², respectively) to the TiO₂ surface (Fig. 2, S1a and S1b) thus indicating that mfp-3 has a strong affinity for TiO₂. COL1A1 showed adsorption to the mfp-3f and mfp-3s films pre-adsorbed to the TiO₂ surfaces and the total mass of the COL1A1/mfp-3f and COL1A1/mfp-3s adsorbed aggregates was $m \sim 252 \pm 2.3$ and $\sim 445 \pm 4.0$ ng/cm², respectively. The adsorption of COL1A1 onto the mfp-3 films resulted in a change in dissipation of the quartz crystal suggesting that the film was less rigid after COL1A1 adsorption. After pH 7.5 buffer (0.1 M phosphate, pH 7.5 and 250 mM salt) was injected into the system, COL1A1/mfp3f or COL1A1/mfp3s precipitated onto the TiO₂ surface ($m \sim 391 \pm 8.6$ and 578.2 ± 8.5 ng/cm², respectively) and the change in dissipation of the quartz crystal suggested that the film was viscoelastic (less rigid).

COL1A1 did not adsorb to the bare TiO₂ surface (Fig. 2 and S1). However, after the addition of mfp-3s to TiO₂ pre-exposed to collagen, the frequency of the TiO₂ coated surface decreased significantly corresponding to a calculated mass of $m = 209 \pm 3.8$ ng/cm². Even though COL1A1 by itself did not adsorb to the bare TiO₂ surface, addition of mfp-3s recruited the COL1A1 in the bulk for co-adsorption to the TiO₂ surface (Fig. 2 and 3). These results show that mfp-3 can be a chaperone for collagen adsorption to surfaces for which it ordinarily doesn't adsorb.

Atomic Force Microscopy (AFM)

The adsorption of COL1A1 to mfp-3 films pre-adsorbed to mica was visualized by AFM. Mfp-3f was deposited onto a freshly cleaved mica surface from bulk solution at pH 3.0 ($C_{\text{mfp3f}} = 20 \mu\text{g/ml}$, $V = 50 \mu\text{L}$) and resulted in complete surface coverage (Fig. 4). Addition of COL1A1 ($C_{\text{COL1A1}} = 25 \mu\text{g/ml}$, $V = 50 \mu\text{L}$) resulted in the formation of a dispersed fibril like structures on the mfp-3f film (Fig. 4b and c). This is in agreement with the QCM-D results that show a strong adsorption of collagen to the mfp-3f or mfp-3s films (Fig. 2).

Surface Forces Apparatus (SFA)

Surface forces between mfp-3s/f and collagen were investigated to quantify the binding strength between COL1A1 and the mussel foot proteins. In contrast to the TiO_2 surface used for QCM studies, SFA analysis was performed with mica. COL1A1 bound to neither surface despite the difference in surface chemistry. The force measurements in the SFA were performed using a sandwich configuration with pre-adsorbed COL1A1 or mfp-3 on both mica surfaces (Fig. 5).

COL1A1 films were deposited on mfp-coated mica at $C_{\text{COL1A1}} = 25 \mu\text{g/mL}$ in 0.1 M sodium acetate, pH 3.0 buffer, which is preferred to prevent the self-assembly of tropocollagen. Attractive and repulsive surface forces were measured between two COL1A1 films on approach and separation of the surfaces (Fig. S5). The bridging interactions between two symmetric mfp-3f/s films mediated by COL1A1 were investigated in the SFA at low pH (~ 3.0) and under physiologically relevant conditions (pH 7.5, 0.25 M KNO_3).

Bridging interaction between mfp-3f films mediated by COL1A1

COL1A1 showed strong adsorption to mfp-3f films on a TiO_2 surface. Here we investigated whether COL1A1 contributed any adhesion to mfp-3f or influenced the cohesion forces between two mfp-3f films.

Strong cohesion was measured between two mfp-3f (hydrophilic variant) protein films in the surface forces apparatus (SFA) (Fig. 5). The mfp-3f films demonstrated a cohesive energy of $W_c = 5.0 \pm 0.2 \text{ mJ/m}^2$ on separation after a compressive contact for short times ($t_c \sim 2 \text{ min}$) (Fig. 5). These results confirm the previous demonstration of mfp-3f cohesion at pH 3.0, and a hardwall of 5 nm is consistent with the hydration diameter of a random coil of mfp-3f [15]. COL1A1 ($C_{\text{COL1A1}} = 25 \mu\text{g/mL}$) enhanced the cohesive energy of interaction between the mfp-3f protein films ($W_c = 7.6 \pm 0.2 \text{ mJ/m}^2$). The increase in hardwall thickness was negligible upon the injection of COL1A1 and is consistent with the AFM data (Fig. 4b), which show that COL1A1 (width of $\sim 1.5 \text{ nm}$), dispersed and intercalated within the mfp-3f films. Similarly, the more hydrophobic variant, mfp-3s, showed a cohesive force ($W_c = 5.4 \pm 0.2 \text{ mJ/m}^2$) for $t_c \sim 2 \text{ min}$, and COL1A1 increased the bridging interactions [16] between the two films ($W_c = 7.2 \pm 0.6 \text{ mJ/m}^2$) (Fig. S4). The increased cohesion between the mfp-3f/s films by COL1A1 probably results from extensive hydrogen bonding, pi-cation and electrostatic interactions between the two proteins (mfp-3f/s and COL1A1).

Bridging adhesion of oxidized Mfp-3f with COL1A1

In previous work demonstrating that Dopa played an essential role in mfp-3 adhesion to mica, Dopa and adhesion were 'knocked out' by periodate oxidation or auto-oxidation at elevated pH [17, 18]. To determine if a similar reliance on Dopa is essential in mediating interactions between mfp-3 and collagen, Dopa was oxidized before the addition of COL1A1 between the mfp-3 films. The previously observed decrease in adhesion after Dopa undergoes auto-oxidation at pH 7.5 [17, 18] was not configurable here due to collagen aggregation at neutral pH. However, under acidic conditions (pH 3.0 and 250 mM salt), strong cohesion was measured between the two mfp-3f films at $t_c \sim 2$ min ($W_c = 4.5 \pm 0.55$ mJ/m²) and $t_c \sim 1$ hr ($W_c = 6.8$ mJ/m²) (Fig. 6a). Increasing the pH of the buffer solution to 7.5 decreased the cohesion between the mfp-3f films by $\sim 80\%$ to $W_c = 1.3 \pm 0.7$ mJ/m² and $W_c = 2.0$ mJ/m² for long and short contact times, respectively. The cohesive energy of the films was not completely abolished suggesting that some of the Dopa in the mfp-3f film was shielded from oxidation or based upon an adhesion independent of Dopa. The long range-repulsion has been attributed to the increased thickness of the protein films due to the stiffening of the mfp-3 backbone caused by quinone tautomerization to dehydroDopa [19]. On reducing the pH back to pH 3.0, the cohesion between the oxidized mfp-3 films increased significantly to $W_c = 4.1 \pm 0.1$ mJ/m² and $W_c = 5.7$ mJ/m² for short and long contact times, respectively.

The pH of the bulk solution was decreased back to pH 3.0 to investigate the effect of COL1A1 on the cohesive interactions between the oxidized mfp-3 films (Fig. 6b). Acidification prevents the precipitation of COL1A1 when added to the gap solution between the mfp-3 films. COL1A1 was added to the gap solution between the oxidized mfp-3f films (Fig 6b) at pH 3.0 and substantial adhesion was measured, $W_{ad} = 5.4 \pm 0.4$ mJ/m² and $W_{ad} = 7.7$ mJ/m², for short and long contact times ($t_c = 2$ and 60 min), respectively. The addition of collagen at pH 3.0 showed high adhesive interaction with the collagen presumably through a bridging interaction between the two mfp-3f coated surfaces despite the partial oxidization of the mfp-3f films. A strong adhesive force was also measured for mfp-3f periodate treated films after the addition of COL1A1 (Fig. S6). The increased but reversible cohesion between the oxidized mfp-3f films by COL1A1 probably arises from extensive hydrogen bonding between the quinone and quinone methide in the oxidized mfp-3s film in addition to the pi-cation and electrostatic interactions between the two proteins (Fig. 7). This cohesion is in stark contrast to the restoration of tendon cohesion by treatment with a di-catechol, nordihydroguaiaretic acid (NDGA), in which case restoration required oxidation of the catechol to quinone presumably leading to the formation of covalent cross-links between the collagen and NDGA [20, 21]. The reversibility of cohesion in oxidized mfp-3-COL1A1 platforms suggests that covalent cross-linking does not play a significant role in the short term ($t_c \sim 60$ min), although another SFA study with oxidized mfp-5 reported that covalent cross-linking did occur after a 12-h incubation [22].

Because the collagen mediated increase in bridging cohesion between the mfp-3f (hydrophilic variant) and mfp-3s (hydrophobic variant) was similar (Fig. 5 and S4), hydrophobic interactions would appear to play a minor role in the bonding mechanism between COL1A1 and mfp-3. Given the small difference that Dopa oxidation had on

collagen-mediated adhesive bridging of mfp-3 films, it is possible in principle that the interaction between COL1A1 and mfp-3 is largely independent of Dopa and based on another interaction that has yet to be determined. Our results suggest that extensive H-bonding, π -cation and electrostatic interactions are contributing to the interaction between mfp-3 and COL1A1 (Fig. 7) and is consistent with the current view of interactions between polyphenols and proteins, especially collagens [21, 23].

Conclusion

Collagen binding to mfp-3 was investigated by preparing a molecular 'sandwich' consisting of mfp-3/collagen/mfp-3. Our results demonstrate that collagen type 1 shows excellent adsorption to mfp-3 films. Collagen type 1 enhances the bridging interactions between two un-oxidized mfp-3f/s (hydrophilic/hydrophobic) films by 50%. The similarity in cohesion of sandwiches made from mfp-3s and mfp-3f suggests that hydrophobic interactions play a minor role in bonding COL1A1 to mfp-3. Collagen type 1 is almost equally effective at reversibly bridging the two mfp-3f films regardless of the oxidation state of Dopa. Extensive H-bonding, π -cation and electrostatic interactions between mfp-3 and collagen are proposed. This study gives insights into understanding the interactions between collagen type-1 and mfps rich in Dopa for the inspiration and design of improved medical and dental adhesives.

Materials and Methods

Mussel foot proteins and collagen

Purification of Mcfp-3f and Mcfp-3s—Mfp-3f and Mfp-3s were purified from the plaques of the California mussels, *Mytilus californianus* respectively as described elsewhere.¹ About 1000 accumulated plaques were thawed and homogenized in a small volume (5 ml/200 plaques) of 5% acetic acid (v/v) containing 8 M urea on ice using a small hand-held tissue grinder (Kontes, Vineland, NJ). The homogenate was centrifuged for 30 min at $20,000 \times g$ and 4 °C. The soluble acetic acid/urea plaque extracts were subjected to reverse phase HPLC using a 260×7 -mm RP-300 Aquapore (Applied Biosciences Inc., Foster City, CA), eluted with a linear gradient of aqueous acetonitrile. Eluant was monitored continuously at 230 and 280 nm, and 1-ml fractions containing Mfp-3F and Mfp-3S were pooled and freeze-dried, injected into Shodex-803 column (5 μ m, 8×300 mm), which was equilibrated and eluted with 5% acetic acid in 0.1% trifluoroacetic acid. Eluant was monitored at 280 nm. Sample purity was assessed by acid urea-PAGE, amino acid analysis (pure mfp3s and 3f had dopa contents of 20 mol %), and MALDI time-of-flight mass spectrometry (5–7 KDa). Fractions with pure Mfp-3F and Mfp-3S were freeze-dried and re-dissolved in buffers for further studies. Rat-tail-derived collagen type 1 (COL1A1) was purchased from Sigma and used without further purification. Quality assurance was by SDS PAGE and hydroxyproline content.

Quartz Crystal Microbalance with Dissipation (QCM-D) Monitoring

TiO₂ sensors (Biolin Scientific Inc.) were cleaned by rinsing with 2% SDS, acetone, ethanol and Milli-Q water respectively. The TiO₂ sensors were further cleaned by UV/ozone plasma

for 15 min. The QCM-D measurements were carried out in a Q-Sense E4 system using an open cell in static solution. Samples were deposited into the open cell using a 20-P Pipetman (Eppendorf). Changes in resonance frequency (F) and dissipation (D) of the TiO₂ quartz crystal were recorded to determine the amount of protein adsorbing to the sensor and the viscoelastic properties of the protein film. The TiO₂ crystal was excited at its fundamental frequency of approximately 5 MHz, and changes can be observed at the fundamental frequency ($n=1$) in addition to overtone frequencies ($n=3, 5, 7$ and 11). Readings were taken from overtone frequencies $n=7$ and 9 . The mass of the adhering protein layer (mfp-3 fast, slow and collagen type-1) was calculated using the Sauerbrey relation:

$$\Delta m = -C \bullet \Delta f / n,$$

where C is in $\text{ng Hz}^{-1}\text{cm}^{-2}$ for a 5 MHz quartz crystal and $n = 3, 5, 7, 9$ is the overtone number. Masses were calculated using overtones 7 and 9. Readings taken at the fundamental frequency are not usually used as they are prone to artifacts from the sensor clamp. It has been previously demonstrated that Sauerbrey equation predicts the adsorbed 'hydrated' mass on the QCM-D crystal surface for uniformly deposited material when the energy dissipation is low ($D < 1 \times 10^{-6}$) [24]. The absorbed hydrated mass, m , (Fig. 2) was calculated using Sauerbrey equation since the coverage of mfp-3 and COL1A1 was homogenous (see AFM images in Fig. 4), the energy dissipation was low ($D < 1 \times 10^{-6}$, see Fig. S1), and the frequency change (F) was similar for the different overtones (Fig. S1).

Atomic Force Microscopy

An MFP-3D-Bio Atomic Force Microscope (AFM, Asylum Research) was used to obtain images with an SNL probe (Bruker) under tapping mode at room temperature (22 °C). Mfp-3s and COL1A1 was deposited on a mica surface (area $\sim 1 \text{ cm}^2$) by adsorbing 50 μL of the protein from a 20 $\mu\text{g/ml}$ mfp3s concentration or a 25 $\mu\text{g/ml}$ of COL1A1 concentration in buffer solution at pH 3.0 or 7.5.

Surface Forces Apparatus (SFA)

The adhesion between mfp-3 and collagen type-1 was measured using a SFA (SurForce LLC). The normal force, F between the surface normalized by the surface radius of curvature, R , was measured as a function of the mica-mica separation distance, D and has been described elsewhere [25, 26]. Briefly, freshly cleaved back-silvered mica was glued onto a silica disc with the silver side on to the glue. The surfaces were then incubated in a 20 μL solution of 20 $\mu\text{g/ml}$ of mfp-3f, mfp-3s or 25 $\mu\text{g/ml}$ collagen type-1 for 15 min. The surfaces were then rinsed with pH 3.0 acetate buffer (0.1 M sodium acetate buffer, pH 3.0 and 0.25 M KNO₃) and kept wet in the buffer solution without exposure to air. The surfaces were then mounted in to the SFA. The interaction of the protein film was either measured against a mica surface or against an opposing protein film. To test the effect of collagen type-1 on the interaction between two mica surfaces symmetrically coated with films of mfp3-fast or slow, 50 μL of 25 $\mu\text{g/mL}$ collagen type-1 was injected into the gap between the surfaces.

Supplementary Material

Refer to Web version on PubMed Central for supplementary material.

Acknowledgments

This research was supported by grants from NIH (R01 DE018468). The MRL Central Facilities (which include AFM and QCM) is supported by the MRSEC Program of the NSF under Award No. DMR 1121053; a member of the NSF-funded Materials Research Facilities Network (www.mrfn.org).

References

1. Rojkind M, Giambone MA, Biempica L. Collagen Types in Normal and Cirrhotic Liver. *Gastroenterology*. 1979; 76:710–9. [PubMed: 421999]
2. Riechert K, Labs K, Lindenhayn K, Sinha P. Semiquantitative analysis of types I and III collagen from tendons and ligaments in a rabbit model. *J Orthop Sci*. 2001; 6:68–74. [PubMed: 11289589]
3. Heino J. The collagen family members as cell adhesion proteins. *Bioessays*. 2007; 29:1001–10. [PubMed: 17876790]
4. Bassar PJ, Schneiderman R, Bank RA, Wachtel E, Maroudas A. Mechanical properties of the collagen network in human articular cartilage as measured by osmotic stress technique. *Arch Biochem Biophys*. 1998; 351:207–19. [PubMed: 9515057]
5. Rodeo SA, Arnoczky SP, Torzilli PA, Hidaka C, Warren RF. Tendon-Healing in a Bone Tunnel - a Biomechanical and Histological Study in the Dog. *J Bone Joint Surg Am*. 1993; 75A:1795–803. [PubMed: 8258550]
6. Zhang, MQ.; Rong, MZ. Self-healing polymers and polymer composites. John Wiley & Sons; 2011.
7. Osorio R, Yamauti M, Osorio E, Roman JS, Toledano M. Zinc-doped dentin adhesive for collagen protection at the hybrid layer. *Eur J Oral Sci*. 2011; 119:401–10. [PubMed: 21896058]
8. Koob TJ, Willis TA, Hernandez DJ. Biocompatibility of NDGA-polymerized collagen fibers. I. Evaluation of cytotoxicity with tendon fibroblasts in vitro. *J Biomed Mater Res*. 2001; 56:31–9. [PubMed: 11309788]
9. Klein J. Forces between Mica Surfaces Bearing Adsorbed Macromolecules in Liquid-Media. *J Chem Soc Farad T 1*. 1983; 79:99–118.
10. Yu J, Kan YJ, Rapp M, Danner E, Wei W, Das S, et al. Adaptive hydrophobic and hydrophilic interactions of mussel foot proteins with organic thin films. *P Natl Acad Sci USA*. 2013; 110:15680–5.
11. Lee BP, Messersmith PB, Israelachvili JN, Waite JH. Mussel-Inspired Adhesives and Coatings. *Annu Rev Mater Res*. 2011; 41:99–132. [PubMed: 22058660]
12. Wei W, Yu J, Broomell C, Israelachvili JN, Waite JH. Hydrophobic enhancement of dopa-mediated adhesion in a mussel foot protein. *Journal of the American Chemical Society*. 2012; 135:377–83. [PubMed: 23214725]
13. Höök F, Kasemo B, Nylander T, Fant C, Sott K, Elwing H. Variations in coupled water, viscoelastic properties, and film thickness of a Mefp-1 protein film during adsorption and cross-linking: a quartz crystal microbalance with dissipation monitoring, ellipsometry, and surface plasmon resonance study. *Analytical chemistry*. 2001; 73:5796–804. [PubMed: 11791547]
14. Wei W, Tan Y, Martinez Rodriguez NR, Yu J, Israelachvili JN, Waite JH. A mussel-derived one component adhesive coacervate. *Acta biomaterialia*. 2014; 10:1663–70. [PubMed: 24060881]
15. Anderson TH, Yu J, Estrada A, Hammer MU, Waite JH, Israelachvili JN. The Contribution of DOPA to Substrate–Peptide Adhesion and Internal Cohesion of Mussel-Inspired Synthetic Peptide Films. *Advanced Functional Materials*. 2010; 20:4196–205. [PubMed: 21603098]
16. Das S, Donaldson SH, Kaufman Y, Israelachvili JN. Interaction of adsorbed polymers with supported cationic bilayers. *Rsc Adv*. 2013; 3:20405–11.
17. Yu J, Wei W, Danner E, Israelachvili JN, Waite JH. Effects of Interfacial Redox in Mussel Adhesive Protein Films on Mica. *Adv Mater*. 2011; 23:2362–6. [PubMed: 21520458]

18. Nicklisch SCT, Das S, Rodriguez NRM, Waite JH, Israelachvili JN. Antioxidant Efficacy and Adhesion Rescue by a Recombinant Mussel Foot Protein-6. *Biotechnol Progr.* 2013; 29:1587–93.
19. Rzepecki LM, Waite JH. Alpha, Beta-Dehydro-3,4-Dihydroxyphenylalanine Derivatives - Rate and Mechanism of Formation. *Arch Biochem Biophys.* 1991; 285:27–36. [PubMed: 1899328]
20. Koob TJ, Hernandez DJ. Material properties of polymerized NDGA-collagen composite fibers: development of biologically based tendon constructs. *Biomaterials.* 2002; 23:203–12. [PubMed: 11762839]
21. Covington AD. *Tanning Chemistry: The Science of Leather.* Tanning Chemistry: The Science of Leather. 2009:1–483.
22. Danner EW, Kan YJ, Hammer MU, Israelachvili JN, Waite JH. Adhesion of Mussel Foot Protein Mefp-5 to Mica: An Underwater Superglue. *Biochemistry-US.* 2012; 51:6511–8.
23. Hagerman AE, Butler LG. Tannin-Protein Interactions - Mechanism and Nutritional Significance. *Fed Proc.* 1980; 39:443.
24. Anderson TH, Min YJ, Weirich KL, Zeng HB, Fygenon D, Israelachvili JN. Formation of Supported Bilayers on Silica Substrates. *Langmuir.* 2009; 25:6997–7005. [PubMed: 19354208]
25. Israelachvili J, Min Y, Akbulut M, Alig A, Carver G, Greene W, et al. Recent advances in the surface forces apparatus (SFA) technique. *Rep Prog Phys.* 2010:73.
26. Das S, Banquy X, Zappone B, Greene GW, Jay GD, Israelachvili JN. Synergistic interactions between grafted hyaluronic acid and lubricin provide enhanced wear protection and lubrication. *Biomacromolecules.* 2013; 14:1669–77. [PubMed: 23560944]

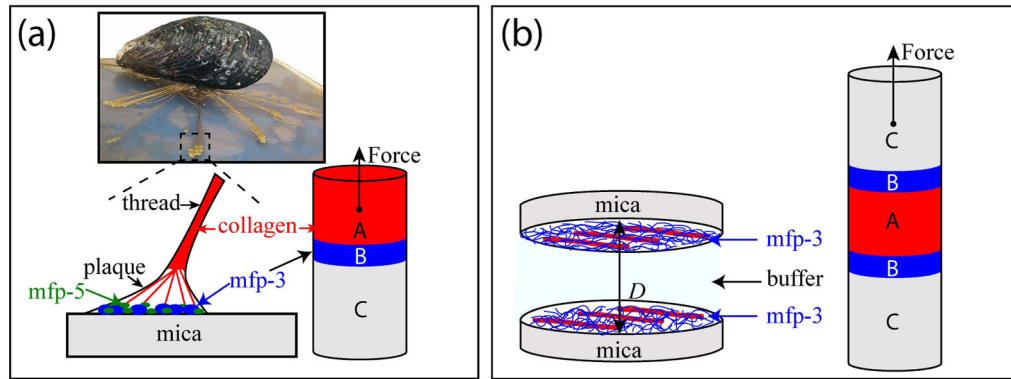


Figure 1.

Studying interactions between collagen and the adhesive proteins from mussels. (a) In mussel byssal threads, collagens known as preCOLs mediate the transfer of load between the mussel plaque and the thread. PreCOLs come within a few nm of the mica surface, thus may bind directly to adhesive mfps such as mfp-3 (blue circles) and mfp-5 (green circles) [11]. (b) The symmetric SFA configuration used in this study to investigate collagen/mfp-3 interactions.

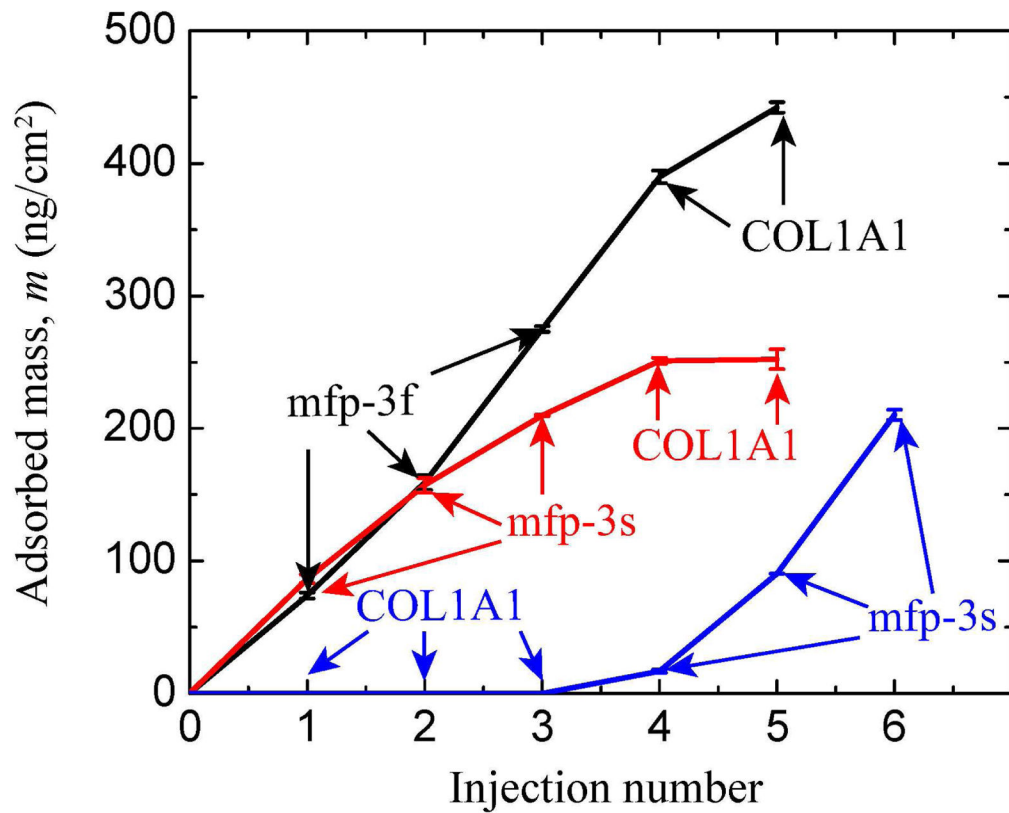


Figure 2.

Quartz crystal microbalance in open cell mode showing relationship between adsorbed *hydrated* mass (calculated from frequency) of mfp-3f, mfp-3s and COL1A1 to a TiO₂ surface and injection number. Injection number refers to the incremental addition of mfp-3 ($C_{\text{mfp-3}} = 20\mu\text{g/ml}$) or COL1A1 ($C_{\text{COL1A1}} = 25\mu\text{g/ml}$) aliquots, which are indicated by arrows for each protein. Note that COL1A1 did not adsorb to TiO₂. Adsorption solution conditions were 0.1 M sodium acetate buffer, pH 3.0 and 0.25 M KNO₃ at room temperature and pressure. For dissipation changes, see supporting data.

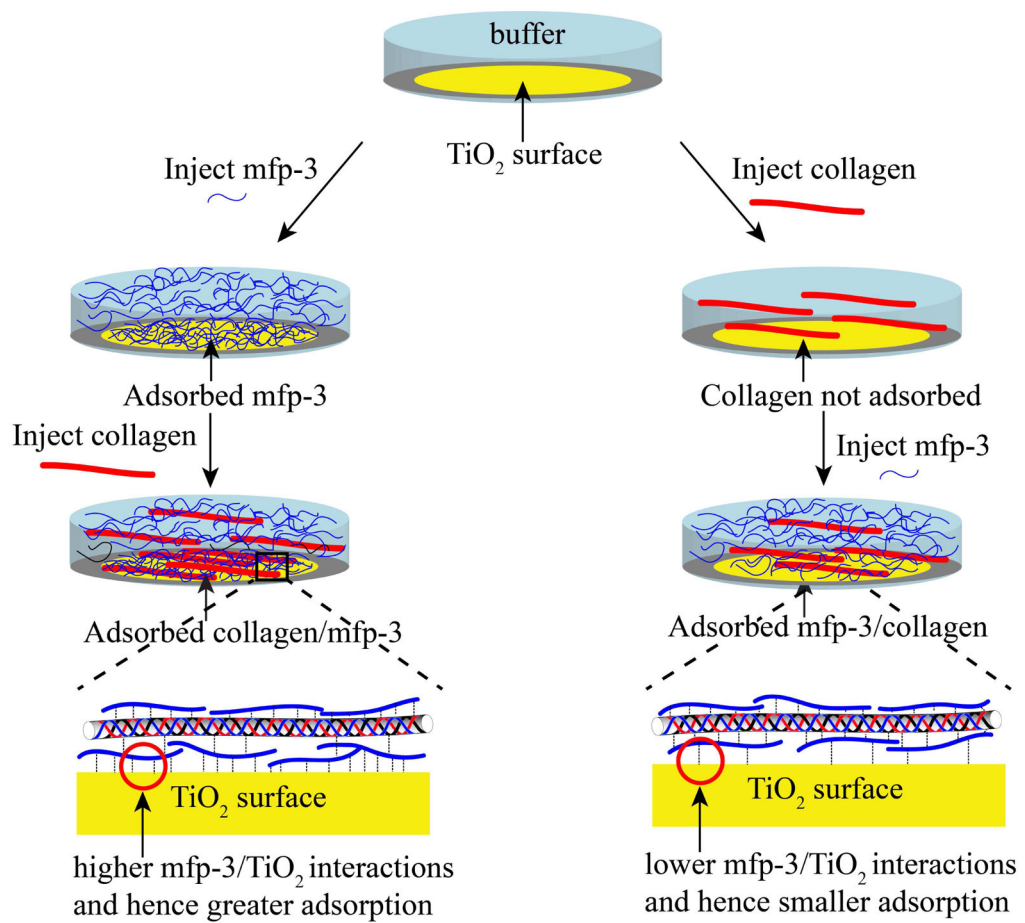


Figure 3. Mechanism of adsorption of COL1A1/mfp-3 to TiO₂. Mfp-3 is pre-adsorbed to TiO₂ before introducing COL1A1 (left), which adsorbs to surface-bound mfp-3. In contrast, COL1A1 by itself is not adsorbed to TiO₂ (right) but can be rescued for adsorption by mfp3-injection. Mfp-3 either binds to COL1A1 creating a sticky complex or to the TiO₂ surface.

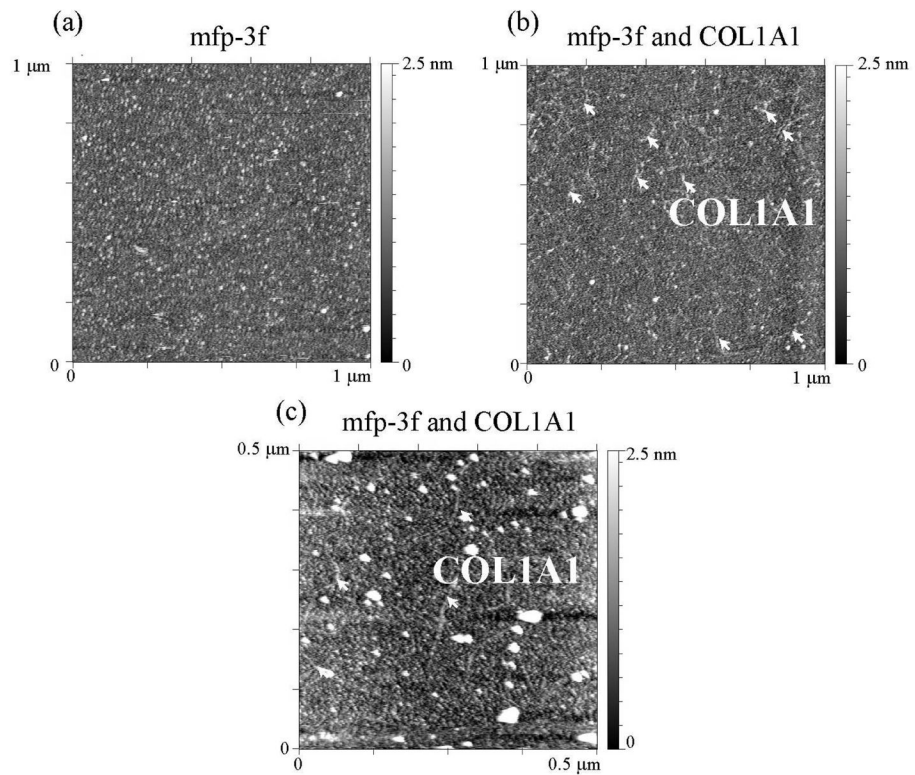
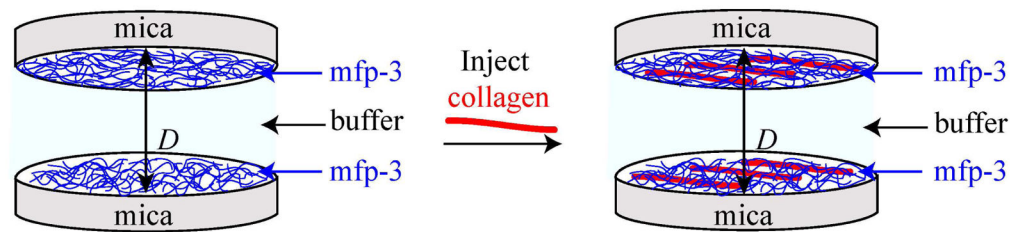
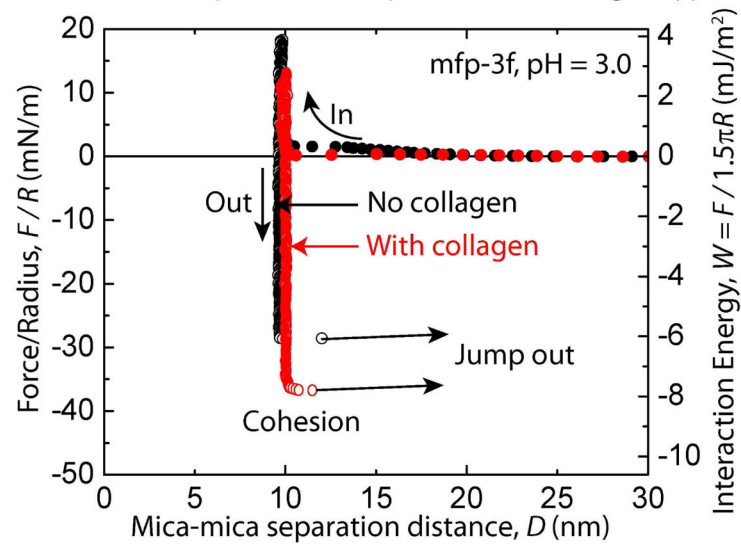


Figure 4.

The topography of mfp-3 on mica and COL1A1 and mfp-3 on mica was measured by AFM. (a) AFM topography image of mfp-3f on mica at pH 3.0. (b) and (c) show topography images of collagen type-1 (COL1A1) deposited onto mica surface coated with mfp-3f in 0.1 M sodium acetate buffer, pH 3.0 and 0.25 M KNO_3 . Expected dimensions of Type 1 α tropocollagen i.e. $\sim 1.5 \text{ nm} \times \sim 300 \text{ nm}$ in agreement with the observed features (arrows).



Interaction of mfp-3 fast vs. mfp-3 fast with collagen type-1

**Figure 5.**

Cohesion between two symmetric mfp-3f films with and without collagen. Representative force vs. distance plots for mfp-3f deposited at $C_{\text{mfp-3f}} = 20 \mu\text{g/mL}$ with collagen ($C_{\text{COL1A1}} = 25 \mu\text{g/mL}$) injected between the two films in 0.1 M sodium acetate buffer, pH 3.0 and 0.25 M KNO_3 .

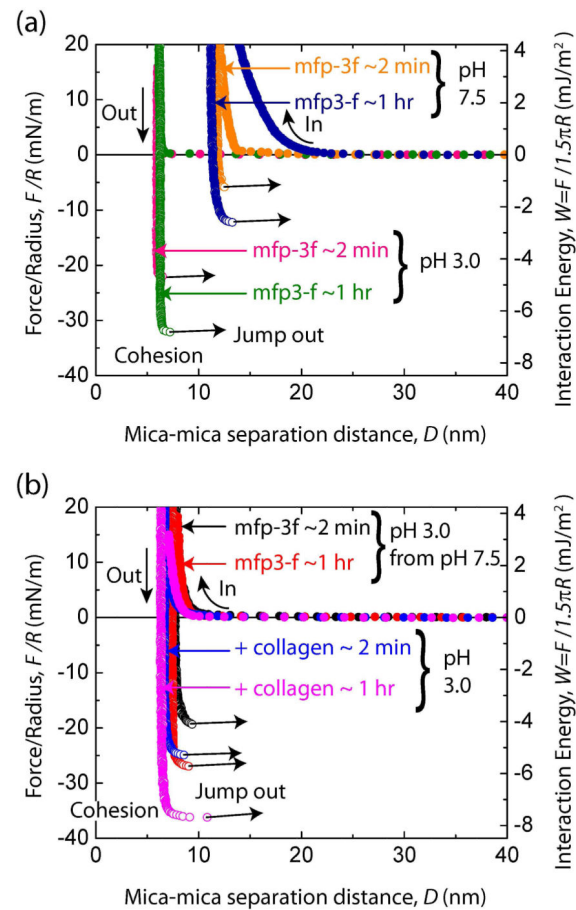


Figure 6.

Bridging cohesion in mfp-3 and the effect of pH and addition of COL1A1. (a)

Representative force vs. distance plots for mfp-3f alone deposited at $C_{\text{mfp-3f}} = 20 \mu\text{g/mL}$ in 0.1 M sodium acetate buffer, pH 3.0 and 0.25 M KNO_3 . (b) Representative force vs. distance plots for mfp-3f in 0.1 M phosphate buffer, pH 7.5 and 0.25 M KNO_3 from pH 3.0 and with collagen ($C_{\text{COL1A1}} = 25 \mu\text{g/mL}$) injected between the two films in 0.1 M sodium acetate buffer, pH 3.0 and 0.25 M KNO_3 .

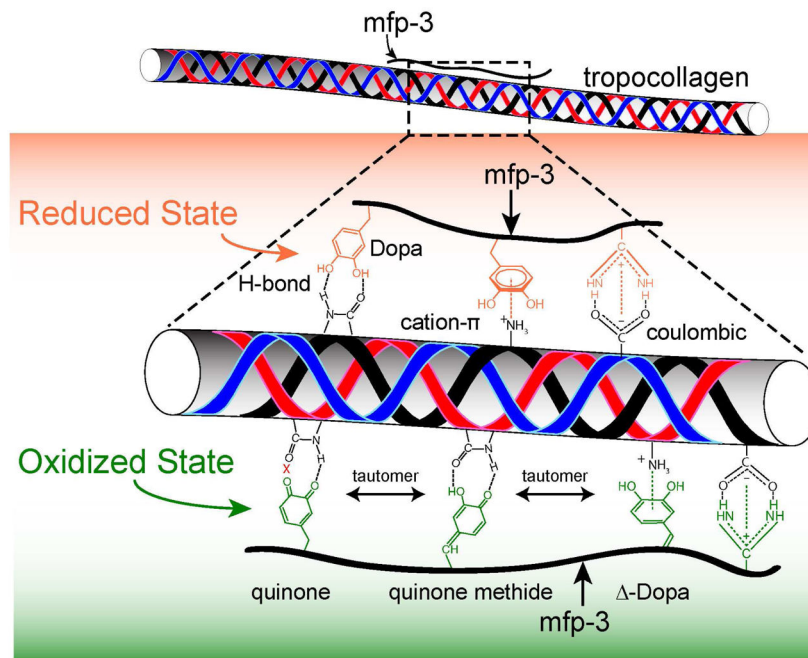


Figure 7. H-bonding and cation- π interactions between collagen and mfp-3 appear to mediate the strong but reversible binding between these molecules. Collagen type-1 deposited onto mfp-3 pre-adsorbed mica surface in 0.1 M sodium acetate buffer, pH 3.0 and 0.25 M KNO_3 .